Optimal operation of distribution networks with high penetration of wind and solar power within a joint active and reactive distribution market environment

Optimal Operation of Distribution Networks with High Penetration of Wind and Solar Power within a Joint Active and Reactive Distribution Market Environment

Rana H.A. Zubo[a,b], Geev Mokryani[a] and Raed Abd-Alhameed[a]
[a]University of Bradford, Bradford BD7 1DP, UK
[b]Kirkuk Technical College, Kirkuk, Iraq
Emails: {r.h.a.zubo, g.mokryani, r.a.a.abd}@bradford.ac.uk

***Abstract*- In this paper, a stochastic approach for the operation of active distribution networks within a joint active and reactive distribution market environment is proposed. The method maximizes the social welfare using market based active and reactive optimal power flow (OPF) subject to network constraints with integration of demand response (DR). Scenario-Tree technique is employed to model the uncertainties associated with solar irradiance, wind speed and load demands.**

It further investigates the impact of solar and wind power penetration on the active and reactive distribution locational prices (D-LMPs) within the distribution market environment. A mixed-integer linear programming (MILP) is used to recast the proposed model, which is solvable using efficient off-the shelf branch-and cut solvers. The 16-bus UK generic distribution system is demonstrated in this work to evaluate the effectiveness of the proposed method.

Results show that DR integration leads to increase in the social welfare and total dispatched active and reactive power and consequently decrease in active and reactive D-LMPs.

***Index terms*— Scenario-based uncertainty modelling, active and reactive distribution market, social welfare maximization, distribution locational marginal prices.**

Index and Sets

i,j	Index of buses
ss	Index of substation
l	Index of loads
w	Index of wind turbines
pv	Index of photovoltaic units
s	Index for scenarios

Parameter

$C_i^{l,P}$	Bid prices of active loads at bus *i*
$C_i^{l,Q}$	Bid prices of reactive loads at bus *i*
$C_i^{DR,P}$	Cost of active power decrement in demand response program at bus *i*
$C_i^{DR,Q}$	Cost of reactive power decrement in demand response program at bus *i*
$\bar{F}_{i,j,s}$	Maximum capacity in branch i-j
$C_i^{w,P}$	Offer prices of WTs active power
$C_i^{PV,P}$	Offer prices of PVs active power
$C_i^{ss,Q}$	Offer prices substation reactive power
$QPF_i^{w,pv}$	Offer prices of WTs and PVs reactive power
Q_{mnd}	Mandatory reactive power of PVs and WTs
Q^{min}	Minimum reactive power of PVs and WTs
Q^{max}	Maximum reactive power of PVs and WTs
Q_{av}	Maximum availability reactive power of PVs and WTs
$C_i^{ss,P}$	Offer prices of substation active power
$f_{j,i,s}$	Current flow in branch *j-i* and scenario *s*
$V_{i,s}^{min}$ / $V_{i,s}^{max}$	Min/Max values of the voltage at bus *i*.
$R_{i,j}$	Resistance of feeders

$X_{i,j}$	Reactance of feeders
M	Large enough positive constant.
X	Reactance of WTs and PVs
m_0	Offered availability price of WTs and PVs
m_1	Offered cost of losses of WTs and PVs
m_2	Offered opportunity cost of WTs and PVs
Z_0,Z_1,Z_2,Z_3	Binary variable related to reactive power payment function of WTs and PVs
π_s	Probability of scenarios
a) Variables	
$P_{i,s}^{l}$	Active power of loads at bus *i* and scenario *s*
$P_{i,s}^{ss}$	Active power of substation at bus *i* and scenario *s*
$P_{i,s}^{w}$	Active power of WTs at bus *i* and scenario *s*
$P_{i,s}^{PV}$	Active power of PVs at bus *i* and scenario *s*
$P_{i,s}^{DR}$	Active power decrement in demand response program at bus *i* and scenario *s*
$Q_{i,s}^{l}$	Reactive power of loads at bus *i* and scenario *s*
$Q_{i,s}^{ss}$	Reactive power of substation at bus *i* and scenario s
$Q_{i,s}^{w}$	Reactive power of WTs at bus *i* and scenario *s*
$Q_{i,s}^{PV}$	Reactive power of PVs at bus *i* and scenario *s*
$Q_{i,s}^{DR}$	Reactive power decrement in demand response at bus *i* and scenario *s*
$u_{i,j}$	Binary utilization variables for feeders
$v_{i,s}$	Voltage at bus *i* and scenario *s*.
V_t	Connection point grid voltage
V_c/I_c	Converter voltage/current

1. INTRODUCTION

1.1. Literature review and motivation

Utilization of renewable energy sources (RES) such as wind turbines (WTs) and photovoltaic (PV) cells are taking substantial attention around the world due to the economic and environmental concerns [1-5]. The intermittent behavior of wind speed and solar irradiance introduces technical challenges such as voltage stability, voltage deviation and power losses to distribution network operators (DNOs) [6, 7]. DNOs have to introduce a reasonable operating strategy to model the uncertainties of electric loads, intermittent power generations of WTs, PVs, and the electricity price. Also, demand response (DR) has been introduced in [8] as an option to mitigate the impact of uncertainties and intermittencies of wind speed and solar irradiance and improving the system's efficiency. DR is defined as the ability of consumers to alter their electricity demand in order to keep the reliability of system [9].

Under the deregulation of electric power systems, the integration of distributed generator (DG) and DR program is becoming the most beneficial way to provide ancillary services in power networks [10-12]. Ancillary services can be defined as a set of services required to support the transmission of electric power from supply to demand to maintain power system security and reliability [13]. Ancillary services are classified as active power ancillary service (load frequency control) and reactive power ancillary service (voltage control) [14]. Most of the researches are carried out about the impact of active power ancillary services as the main services in electricity markets at transmission level; for instance, Ref. [15] illustrates how frequency control constraints can be obtained and involved into a market dispatch algorithm. In [16] a new frequency control market is introduced in order to host frequency response reserve offers from both loads and generators. Ref. [17] introduces the flexible frequency operation strategy of power system with high renewable penetration in order to gain the flexibility of the power grids. Absence of reactive power ancillary services may cause voltage instability all over the power network and lead to voltage collapse which is the main reason of blackouts [18]. Supporting the reactive power ancillary services is considered as a part of distribution network operators' (DNOs) activities.

In general, the reactive power markets can be cleared separately or simultaneously from active power markets. In reactive power markets, the market structure, payment mechanism and pricing model are main factors for determining the appropriate components of reactive power market [19]. Recently, most published papers have discussed the impact of reactive ancillary

services in transmission systems; for example, in [20], a quadratic reactive power cost model for transmission system has been proposed to optimize reactive power procurement. Pay-as-bid pricing mechanism for reactive power market in the transmission system which take into account the local nature of reactive power during the clearing of reactive power has been introduced in [21]. In [22] active and reactive power markets at transmission level are implemented to present an interaction between energy market and reactive markets.

However, a few papers have discussed the reactive power market at distribution level. For instance, in [23], a settlement procedure for reactive power market for DGs in distribution systems has been proposed for reactive/voltage ancillary services to minimize reactive power payment by DNOs. Ref [24] discusses the application of a sustainable operational scheduling method which systemamically focuses on a day-ahead active and reactive power markets at distribution level in order to dispatch active and reactive powers in distribution systems with WTs. The opreration of distribution networks within reactive power market still suffers from lack of attention in the exisiting studies on. In addition, these studies did not consider the joint active and reactive power market model at distribution level to maxmize the social welfare (SW). Table 1 provides a comprehensive comparison of the exisiting studies and the proposed method. This paper proposes a methodology for operation of distribution network within a novel joint active and reactive power market at distribution level with integration of DR. A stochastic approach is used to evaluate the amount of wind and solar power penetration on the SW and active and reactive distribution locational marginal prices (D-LMPs) taking into account the uncertainties related to wind speed, solar irradiance, and load demand.

Table 1. Comparison of the proposed method with existing ones

Reference	Transmission or distribution level	Renewable energy sources	Correlation	DR	Power market		SW
					Active	Reactive	
[6]	Transmission	Yes	Yes	Yes	Yes	No	No
[7]	Transmission	Yes	No	No	Yes	No	No
[8]	Transmission	Yes	No	Yes	Yes	No	No
[9]	Distribution	No	No	Yes	Yes	No	Yes
[12-13-14]	Transmission	Yes	No	No	Yes	No	No
[16-17-18]	Transmission	No	No	No	No	Yes	No
[19]	Transmission	No	No	No	Yes	Yes	No
[20-21, 24]	Distribution	Yes	No	No	Yes	Yes	No
Proposed method	**Distribution**	**Yes**	**Yes**	**Yes**	**Yes**	**Yes**	**Yes**

1.2. Contributions

To the best of our knowledge, none of the above studies introduced a stochastic approach for the operation of distribution networks within the proposed joint active and reactive power market model by maximizing the social welfare which is the gap that this work aims to fill it.

In summary, the main contributions of this paper are listed as follows:

- To propose an MILP optimization approach for operation of distribution networks within a proposed joint active and reactive distribution with integration of DR.
- To design and develop a joint active and reactive electricity market model at distribution level.
- To model the correlated uncertainties associated with wind speed, solar irradiation and load demand using Scenario-Tree approach.

1.3. Paper organization

The rest of this paper is organized as follows. Section 2 discusses the uncertainty modeling. Section 3 discusses the proposed distribution market model and formulation. Section 4 presents case study (16-bus UKGDS) and simulation results, while Section 5, discusses the simulation results. Conclusion and future work are presented in Section 6.

2. UNCERTAINTY MODELING

2.1. Wind speed modelling

Generally, the variation of wind speed is modelled using Weibull probability density function (PDF)[25-27]. The PDF function which relates the wind speed and the output power of WTs is given by [28].

$$PDF(v) = (\frac{k}{c})(\frac{v}{c})^{k-1} \exp\left[-(\frac{v}{c})^{k} \right] \quad (1)$$

where v is wind speed, c is the scale index of the Weibull PDF of wind speed and k is the shape index. Hence, the generated power of WTs can be determined by using its power curve as follows [29-31]:

$$P_w(v)=\begin{cases}0, & 0\le v\le v_{ci}\\ P_{rated}\times\dfrac{v-v_{ci}}{v_r-v_{ci}}, & v_{ci}\le v\le v_r\\ P_{rated}, & v_r\le v\le v_{co}\\ 0, & v_{co}\le v\end{cases} \quad (2)$$

where P_w is the generated power of WTs, P_{rated} is the rated power, v_{ci} is the cut-in speed, v_r is rated speed and v_{co} is cut-off speed. Fig (1) shows the speed power curve of WTs.

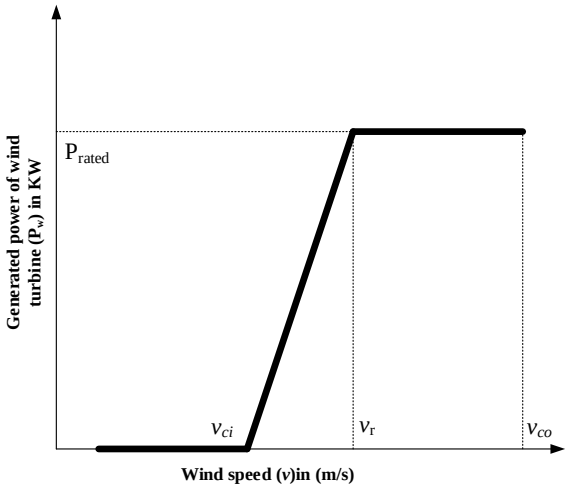

Fig (1) the idealised power curve of a wind turbine

The active and reactive wind power at bus *i* and scenario *s* are calculated as follows:

$$0\le P_{i,s}^{w}\le\gamma_{i,s}^{w}\times P_{i,rated}^{w} \quad (3)$$

where $\gamma_{i,s}^{w}$ is the percentage of active and reactive power generated by WTs at scenario *s*.

2.2. Solar irradiance modelling

The solar irradiance is modeled using Beta PDF which is described as follows:

$$PDF(s)=\begin{cases}\dfrac{\Gamma(\alpha+\beta)}{\Gamma(\alpha)+\Gamma(\beta)}\times s^{\alpha-1}\times(1-s)^{\beta-1}, & 0\le s\le 1, 0\le\alpha,\beta\\ 0 & else\end{cases} \quad (4)$$

where *s* represents the solar irradiance (kW/m^2). α and β which are the parameters of Beta PDF are derived as follows:

$$\beta=(1-\mu)\times\left(\frac{\mu\times(1-\mu)}{\sigma^2}-1\right) \quad (5)$$

$$\alpha=\frac{\mu\times\beta}{1-\mu} \quad (6)$$

where μ and σ are the mean and standard deviation of the random variable. Eqs. (7) and (8) are used to estimate the output power of PV, the solar irradiance and the cell temperature as follow [32, 33]:

$$P_{pv}=P_{STC}\left\{\frac{G}{1000}\left[1+\delta\left(T_{cell}-25\right)\right]\right\} \quad (7)$$

$$T_{cell}=T_{amb}+\left(\frac{NOCT-20}{800}\right)G \quad (8)$$

where $P_{pv}$is the output power in MW, P_{STC} is the power under standard test condition in MW, δ is the power- temperature coefficient in (%/°C), T_{cell} is the cell temperature in °C, T_{amb} is the ambient temperature in °C, $NOCT$ are the national operating cell temperature conditions in °C, G ,is the solar irradiance in (W/m^2).

2.3. Load demand uncertainty modeling

Normal PDF is used to model load demands at each bus. The PDF of the normal distribution for uncertain load l is [34-36]:

$$PDF(l) = \frac{1}{\sigma_l \sqrt{2\pi}} \times \exp\left[-\left(\frac{(l-\mu_l)^2}{2\sigma_l^2} \right) \right] \quad (9)$$

where μ_l and σ_l are the mean and standard deviation, respectively.

2.4. Modelling approach

In this section, based on "duration curve" [37-40], the model of the correlated uncertainties related to wind speed, solar irradiance and load demand are obtained by the cumulative distribution function (CDF) for each block. The procedure is the following:

- The historical data for hourly demand, wind speed and solar irradiation must be available in order to present the model. Historical data of wind speed and solar irradiance for 8760 hours are described in Fig. 2, which are used in the same period as load demand. Historical data are separated into load demand, wind speed and solar irradiation, respectively, in order to obtain the factorized data.
- The obtained factorized data are used to build the load demand curve which are arranged from higher to lower values keeping the correlation between the different hourly data of load demand, wind speed and solar irradiance as shown in Fig.2
- Time blocks are set to determine the load duration curve and its length varies along the load duration in order to carefully consider the load demand in the model. For each time block load demand, wind speed and solar irradiance are arranged in descending order.
- The CDF of the load demand, wind and PV factors is calculated for each block.
- Each CDF is divided into segments with their associated probability (i.e. number of demand levels which can achieved in every time block).
- The scenarios are formulated for each time block by combination of the levels of uncertain data. Thus, for each load level *ll*, each scenario *s* comprises an average demand factor $\mu_{ll,s}^{D}$, a maximum level of wind power $\mu_{ll,s}^{w}$ and the maximum level of PV power $\mu_{ll,s}^{\theta}$.
- The total number of scenarios is 108, which was obtained by multiplication of four time blocks, three load demand levels, three wind speed levels, three solar irradiation levels (4×3×3×3=108).
- It should be note that the model is applicable for all periods of the day.

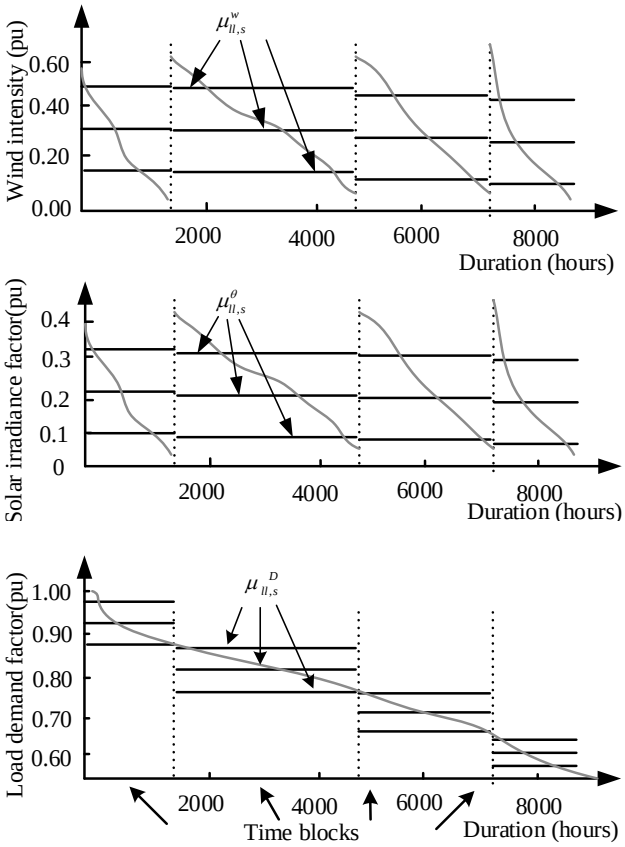

Fig.2. Load demand, wind speed, solar irradiance and offer prices of wind and PV curves and levels

3. JOINT ACTIVE AND REACTIVE DISTRIBUTION MODEL AND FORMULATION

A joint active and reactive market model at distribution level is proposed in this section. The structure of proposed market is based on bilateral contracts and pool within DNOs control zone, which is shown in Fig.3. In this market model, the DNO acts as the operator of the distribution market where it manages the operational facilities and buying active and/or reactive power through the pool or from bilateral contracts. Dispatchable loads (DLs), WTs and PVs send offers and bids prices of active and reactive power in form of blocks to the distribution market every hour. Then, the DNO combines offers and bids prices in order to maximize the consumers' benefit function while minimizing the cost of energy and which is called maximizing social welfare [41].

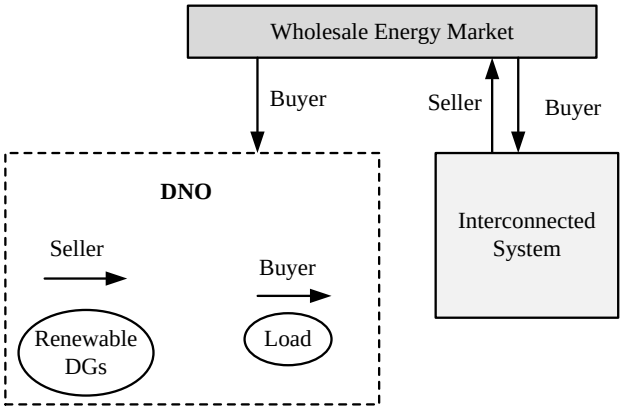

Fig.3.The structure of the DNO acquisition market

The following actions are carried out by the proposed market:

1) A day-ahead schedule of WTs, PVs and DLs according to the market prices. In every trade day, WTs, PVs and DLs provide offer and bid prices and active and reactive power quantity information for every 24-hour trading period one day ahead. For every trading duration the dispatch schedules are determined [41].
2) An adjustment market, which closes a few hours earlier before delivery and allows adjustment in correction due to unexpected supply-demand imbalances occurred during the day due to load or generation variations.

3) A real-time intraday optimization operation for economic requirements and operation is done by changing scheduling every 15-minutes (balancing market).

In this distribution market, active and reactive power, which are produced by wind and solar, contributes to the pool including the three consecutive and autonomous short-term trading floors as explained above. In the day-ahead market, to eliminate or reduce the variation between the amount of energy cleared and the expected generation, the processes carried out in the adjustment and real time distribution markets are required. In the adjustment market, wind and solar producers are allowed to update their estimated generation in their offers, which is lead to reduce the related uncertainties. Imbalances at real time between generation and demand are settled at balancing market in order to ensure that the electricity demand equals to electricity supply in real time [42].

Under the proposed distribution market, market clearing quantity price and quantity are calculated by maximizing SW taking into consideration network constraints with integration of DR. The optimization problem is formulated in the following as the sum of the total consumers' benefits minus the sum of DR cost and the sum of the total generation costs (substation, WTs and PVs).

$$\begin{aligned}\text{Maximize SW} = &\left(\sum_{i=1}^{NB}\sum_{s=1}^{NS}\pi_s C_i^{l,P}P_{i,s}^{l}+\sum_{i=1}^{NB}\sum_{s=1}^{NS}\pi_s C_i^{l,Q}Q_{i,s}^{l}\right)\\ &-\left(\sum_{i=1}^{NB}\sum_{s=1}^{NS}C_i^{DR,P}P_{i,s}^{DR}+\sum_{i=1}^{NB}\sum_{s=1}^{NS}C_i^{DR,Q}Q_{i,s}^{DR}\right)\\ &-\left(\begin{array}{l}\sum_{i=1}^{NB}\sum_{s=1}^{NS}C_i^{ss,P}P_{i,s}^{ss}+\sum_{i=1}^{NB}\sum_{s=1}^{NS}C_i^{ss,Q}Q_{i,s}^{ss}\\ +\sum_{i=1}^{NB}\sum_{s=1}^{NS}\pi_s C_i^{w,P}P_{i,s}^{w}+\sum_{i=1}^{NB}\sum_{s=1}^{NS}\pi_s C_i^{pv,p}P_{i,s}^{pv}\\ +\sum_{i=1}^{NB}QPF_i^{w,pv}\end{array}\right)\end{aligned} \tag{10}$$

subject to

-Kirchhoff's current law

$$\sum P_{i,s}^{ss}+\sum P_{i,s}^{w}+\sum P_{i,s}^{pv}+\sum P_{i,s}^{DR}-\sum P_{i,s}^{l}=f_{i,j,s}-f_{j,i,s} \tag{11}$$

$$\sum Q_{i,s}^{ss}+\sum Q_{i,s}^{w}+\sum Q_{i,s}^{pv}+\sum Q_{i,s}^{DR}-\sum Q_{i,s}^{l}=f_{i,j,s}-f_{j,i,s} \tag{12}$$

-Kirchhoff's voltage law

$$u_{i,j}\left[R_{i,j}f_{i,j,s}-(v_{i,s}-v_{j,s})\right]=0 \tag{13}$$

$$u_{i,j}\left[X_{i,j}f_{i,j,s}-(v_{i,s}-v_{j,s})\right]=0 \tag{14}$$

-Active and reactive power capacity constraints at substation

$$P_i^{ss,\min}\le P_{i,s}^{ss}\le P_i^{ss,\max} \tag{15}$$

$$Q_i^{ss,\min}\le Q_{i,s}^{ss}\le Q_i^{ss,\max} \tag{16}$$

-Active power capacity constraints of WTs and PVs

$$P_i^{w,\min}\le P_{i,s}^{w}\le P_i^{w,\max} \tag{17}$$

$$P_i^{pv,\min}\le P_{i,s}^{pv}\le P_i^{pv,\max} \tag{18}$$

-Voltage and current constraint at each bus

$$V_i^{\min}\le V_{i,s}\le V_i^{\max} \tag{19}$$

$$-u_{i,j}\bar{F}_{i,j}\le f_{i,j,s}\le u_{i,j}\bar{F}_{i,j} \tag{20}$$

-DR constraints

$$0\le P_{i,s}^{DR}\le P_i^{DR,\max} \tag{21}$$

$$0\le Q_{i,s}^{DR}\le Q_i^{DR,\max} \tag{22}$$

The objective function (10) consists of three terms: 1) consumer benefit, 2) DR cost, (3) generation cost (substation and WTs and PVs). In the proposed market, reactive power offer price of substation is assumed to be fixed. The Kirchhoff's current and voltage laws are represented in (11)-(14) respectively. The binary variable $u_{i,j}$ is related with every feeders in order to model its

utilization. Constraints (15) and (16) set the upper bounds for the substation active and reactive power. The active power which is supplied by WTs and PVs are limited by the minimum between their capacities and the maximum power availability in (17) and (18). WTs' and PVs' power limits depend on wind speed and solar irradiance. Upper and lower limits in (19) and (20) represent the voltage and current constraints at each bus respectively. DR constraints have been introduced in Equations (21) and (22).

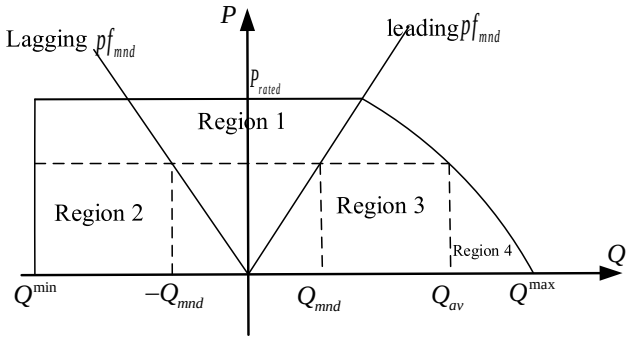

a) capability curve of renewable DGs

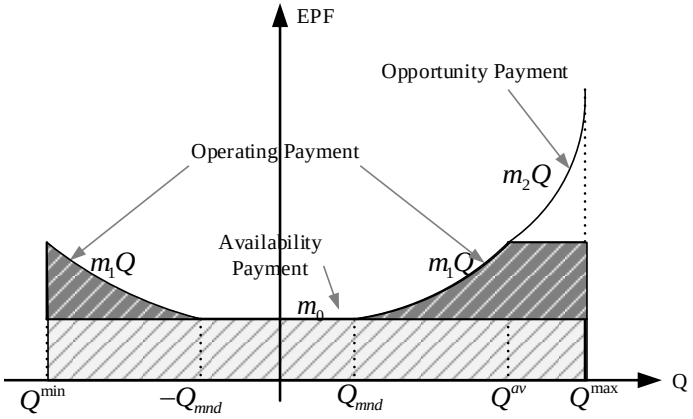

b) reactive power offer structure

Fig.4 a) Reactive power capability curve, b) reactive power offer structure

3.1. Reactive power offer structure

Based on the capability curve of WTs and PVs shown in Fig. (4a), reactive power payment structure is divided into four regions[24, 43] as follows:

Region 1(-Q_{mnd} to Q_{mnd}), Region 2(Q^{min} to $-Q_{mnd}$), Region 3 (Q_{mnd} to Q_{av}) and Region 4 (Q_{mnd} to Q^{max}): when WTs and PVs operate in region 1, it should receive only the payment (m_0) which is called availability payment. In regions 2 and 3, WTs and PVs should receive the availability and losses payments, because WTs and PVs in these regions will lose extra active power losses.

In region 4, the reactive power payment function should contain three payments, which are availability payment, losses payment and opportunity payment as the WTs and PVs lose the opportunity to sell active power. Eq. (23) defines the maximum available reactive power, which is supply by WTs and PVs. The capability curve of WTs and PVs is defined in Eq. (24). Based on the above classification of reactive power production payment, the reactive power payment (QPF) of WTs and PVs in these regions can be formulated as in Eq. (25). Note that the opportunity offer of Q is a quadratic function.

$$Q = \left\{ \begin{array}{l} \sqrt{\left(V_t\, I_c\right)^2 - \left(P^{w,pv}\right)^2} \\ \sqrt{\left(\frac{V_t\, V_c}{X_c}\right)^2 - \left(P^{w,pv}\right)^2} - \frac{V_t^2}{X_c} \end{array} \right\} \qquad (23)$$

$$QPF=\begin{cases} m_0 & -Q_{mnd}\le Q_i^{w,pv}\le Q_{mnd} \\ \frac{1}{2}m_1\left((Q_1)^2-(Q_{mnd})^2\right) & Q_1\le Q_i^{w,pv}\le -Q_{mnd} \\ \frac{1}{2}m_1\left((Q_2)^2-(Q_{mnd})^2\right) & Q_{mnd}\le Q^{w,pv}\le Q_2 \\ \left(\frac{1}{2}m_1\left((Q_{av})^2-(Q_{mnd})^2\right)+\right. & \\ \left.\frac{1}{2}m_2\left((Q_3)^2-(Q_{av})^2\right)\right) & Q_{mnd}\le Q^{w,pv}\le Q_{av}, Q_{av}\le Q^{w,pv}\le Q_3 \end{cases} \quad (24)$$

$$QPF=Z_0m_0+Z_1\frac{1}{2}m_1\left((Q_1)^2-(Q_{mnd})^2\right)$$
$$+Z_2\frac{1}{2}m_1\left((Q_2)^2-(Q_{mnd})^2\right) \quad (25)$$
$$+Z_3\left[\frac{1}{2}m_1\left((Q_{av})^2-(Q_{mnd})^2\right)+\frac{1}{2}m_2\left((Q_3)^2-(Q_{av})^2\right)\right]$$

where Z_0,Z_1,Z_2 and Z_3 are the binary variables which determine the compensation region of WTs and PVs. If the accepted unit is operated in region 1, then Z_o=1 and Z_1=Z_2=Z_3=0, in region 2, Z_0=Z_1=1 and Z_2=Z_3=0, in region 3, Z_0=Z_2=1 and Z_1=Z_3=0, in region 4, Z_0=Z_2=Z_3=1 and Z_1=0. Fig.4.b illustrates the QPF as function of reactive power generated by WTs and PVs.
The equality and inequality constraints of WTs and PVs are given as follow

$$Z_0,Z_1,Z_2,Z_3\in\{0,1\} \quad (26)$$
$$-Z_0Q_{mnd}^{w,pv}\le Q_0^{w,pv}\le Z_0Q_{mnd}^{w,pv} \quad (27)$$
$$Z_1Q_{\min}^{w,pv}\le Q_1^{w}\le -Z_1Q_{mnd}^{w,pv} \quad (28)$$
$$Z_2Q_{mnd}^{w,pv}\le Q_2^{w,pv}\le Z_2Q_{av}^{w,pv} \quad (29)$$
$$Z_3Q_{av}^{w,pv}\le Q_3^{w,pv}\le Z_3Q_{\max}^{w,pv} \quad (30)$$
$$Q_{mnd}^{w,pv}=P^{W,PV}\tan\left(\cos^{-1}\left(pf_{mnd}\right)\right) \quad (31)$$
$$Q^{w,pv}=Q_0^{w,pv}+Q_1^{w,pv}+Q_2^{w,pv}+Q_3^{w,pv} \quad (32)$$
$$Z_1+Z_2+Z_{3,}\le Z_0 \quad (33)$$

In order to minimize the reactive power dispatch impact on the initial active power of WTs and PVs, a cap on the reduction in the active power is imposed.

$$\Delta P_i^{w,pv}\le x_i^{w,pv}P_i^{w,pv,\text{int}} \quad (34)$$

where $x_i^{w,pv}$ is the considered cap on reduction of active power of WTs and PVs.

Note that the total reactive payment function QPF is nonlinear. In order to keep the problem linear, the quadratic function in (25) is linearized by piecewise linearization approach as in Eq. (37 to 41) in below section.

3.2. Linearization model

The proposed optimization problem is nonlinear, therefore, finding the global optimal solution is hard to obtain. The below linearization model was first proposed by Haffner et al. [44] which have been successfully implemented in [38]. The linearized network model is an adapted version of the dc model that is based on two assumptions: (i) all current injections and flows have the same power factor, and (ii) the per-unit voltage drop across a branch is equal to the difference between the per-unit magnitudes of the nodal voltages at both ends of the branch. Assumption (i) allows expressing Kirchhoff's current law as a set of linear scalar equalities in terms of current magnitudes. In addition, assumption (ii) allows formulating Kirchhoff's voltage law for branches in use as a linear expression relating the magnitudes of currents, nodal voltages, and branch impedances. The equivalent integer linear reformulation is shown in (35) and (36), where M is a large enough positive constant and its impact is similar to eq. (13) and (14).

$$-M(1-u_{i,j})\le R_{i,j}f_{i,j,s}-(v_{i,s}-v_{j,s})\le M(1-u_{i,j}) \quad (35)$$
$$-M(1-u_{i,j})\le X_{i,j}f_{i,j,s}-(v_{i,s}-v_{j,s})\le M(1-u_{i,j}) \quad (36)$$

$u_{i,j}$ is binary utilization variables for all feeders.
The linearization of the nonlinear formulation of QPF is carried out using piecewise linearization approach [45]. Equations (37)-(41) describe the linearization process as follows:

$$Q^2 = \sum_{l=1}^{L} (2l-1)\frac{Q^{\max}}{L}\Delta Q_l \quad (37)$$

$$Q = Q^{(+)} - Q^{(-)} \quad (38)$$

$$Q^{(+)} \geq 0; \;\; Q^{(-)} \geq 0 \quad (39)$$

$$Q^{(+)} + Q^{(-)} = \sum_{l=1}^{L} Q_l \quad (40)$$

$$\Delta Q_l \geq \Delta Q_{l+1} \quad (41)$$

In equation (37), the quadratic variable is linearized through piecewise linear approximation considering L number of segments. Q is divided into two parts, forward variable and reverse auxiliary flow variables so that it will only use the first quadrant of the quadratic curve as explained in equation (38). It is worth mentioning that these variables cannot be nonzero and non-negative simultaneously as imposed by (39). Equation (40) guarantees that the step flow variables ΔQ_l equals to the flow. Equation (41) guarantees the successive filling of the partitions.

4. CASE STUDY

The following case study is based on 33kV, 16-bus UK generic distribution system (UKGDS)[46]. It is assumed that two WTs of 630kW are installed at the buses 6 and 11 and one PV unit of 220kW at the bus 13. The assumed limits for voltage were between V_{max}= 1.06 p.u and V_{min}=0.94 p.u. WTs and PV power factor was assumed to be 0.95 lagging. The total peak demand for active is 38.2MW and 7.7 MVAr for reactive power. Active and reactive offer price of substation are 150 £/MWh and 70 £/MVArh, respectively. The active and reactive cost of DR program paid to the customers to reduce their active and reactive load demand for 3% at each bus is assumed to be 10 £/MWh and 5 £/ MVArh, respectively. The single-line diagram of the 16-bus UKGDS is shown in Fig. 5. Table 2 provides the characteristics of load demand, wind speed and solar irradiance scenarios. Bid prices for active and reactive load demands are presented in Tables 3 and 4 respectively. It is assumed that for each load at maximum demand there are three blocks [47, 48].

The proposed mix integer linear programming (MILP) problem has been simulated in General Algebraic Modelling System (GAMS) environment and solved by CPLEX solver [49] on a PC with Core i7 CPU and 16 GB of RAM.

Table 2 Scenarios

Number of Scenarios	Demand block	Number of Hours	Demand level	Wind	Solar	Number of Scenarios	Demand block	Number of Hours	Demand level	Wind	Solar
1	1	1200	0.967	0.436	0.336	55	3	2400	0.793	0.365	0.265
2	1	1200	0.967	0.436	0.167	56	3	2400	0.793	0.365	0.223
3	1	1200	0.967	0.436	0.102	57	3	2400	0.793	0.365	0.092
4	1	1200	0.967	0.267	0.336	58	3	2400	0.793	0.223	0.265
5	1	1200	0.967	0.267	0.167	59	3	2400	0.793	0.223	0.223
6	1	1200	0.967	0.267	0.102	60	3	2400	0.793	0.223	0.092
7	1	1200	0.967	0.122	0.336	61	3	2400	0.793	0.112	0.265
8	1	1200	0.967	0.122	0.167	62	3	2400	0.793	0.112	0.223
9	1	1200	0.967	0.122	0.102	63	3	2400	0.793	0.112	0.092
10	1	1200	0.921	0.436	0.336	64	3	2400	0.755	0.365	0.265
11	1	1200	0.921	0.436	0.167	65	3	2400	0.755	0.365	0.223
12	1	1200	0.921	0.436	0.102	66	3	2400	0.755	0.365	0.092
13	1	1200	0.921	0.267	0.336	67	3	2400	0.755	0.223	0.265
14	1	1200	0.921	0.267	0.167	68	3	2400	0.755	0.223	0.223
15	1	1200	0.921	0.267	0.102	69	3	2400	0.755	0.223	0.092
16	1	1200	0.921	0.122	0.336	70	3	2400	0.755	0.112	0.265
17	1	1200	0.921	0.122	0.167	71	3	2400	0.755	0.112	0.223
18	1	1200	0.921	0.122	0.102	72	3	2400	0.755	0.112	0.092
19	1	1200	0.875	0.436	0.336	73	3	2400	0.717	0.365	0.265
20	1	1200	0.875	0.436	0.167	74	3	2400	0.717	0.365	0.223
21	1	1200	0.875	0.436	0.102	75	3	2400	0.717	0.365	0.092
22	1	1200	0.875	0.267	0.336	76	3	2400	0.717	0.223	0.265
23	1	1200	0.875	0.267	0.167	77	3	2400	0.717	0.223	0.223
24	1	1200	0.875	0.267	0.102	78	3	2400	0.717	0.223	0.092
25	1	1200	0.875	0.122	0.336	79	3	2400	0.717	0.112	0.265
26	1	1200	0.875	0.122	0.167	80	3	2400	0.717	0.112	0.223
27	1	1200	0.875	0.122	0.102	81	3	2400	0.717	0.112	0.092
28	2	3600	0.873	0.401	0.301	82	4	1560	0.682	0.351	0.251
29	2	3600	0.873	0.401	0.223	83	4	1560	0.682	0.351	0.174
30	2	3600	0.873	0.401	0.102	84	4	1560	0.682	0.351	0.085
31	2	3600	0.873	0.223	0.301	85	4	1560	0.682	0.194	0.251
32	2	3600	0.873	0.223	0.223	86	4	1560	0.682	0.194	0.174
33	2	3600	0.873	0.223	0.102	87	4	1560	0.682	0.194	0.085
34	2	3600	0.873	0.122	0.301	88	4	1560	0.682	0.095	0.251
35	2	3600	0.873	0.122	0.223	89	4	1560	0.682	0.095	0.174
36	2	3600	0.873	0.122	0.102	90	4	1560	0.682	0.095	0.085
37	2	3600	0.831	0.401	0.301	91	4	1560	0.649	0.351	0.251
38	2	3600	0.831	0.401	0.223	92	4	1560	0.649	0.351	0.174
39	2	3600	0.831	0.401	0.102	93	4	1560	0.649	0.351	0.085
40	2	3600	0.831	0.223	0.301	94	4	1560	0.649	0.194	0.251
41	2	3600	0.831	0.223	0.223	95	4	1560	0.649	0.194	0.174
42	2	3600	0.831	0.223	0.102	96	4	1560	0.649	0.194	0.085
43	2	3600	0.831	0.122	0.301	97	4	1560	0.649	0.095	0.251
44	2	3600	0.831	0.122	0.223	98	4	1560	0.649	0.095	0.174
45	2	3600	0.831	0.122	0.102	99	4	1560	0.649	0.095	0.085
46	2	3600	0.789	0.401	0.301	100	4	1560	0.617	0.351	0.251
47	2	3600	0.789	0.401	0.223	101	4	1560	0.617	0.351	0.174
48	2	3600	0.789	0.401	0.102	102	4	1560	0.617	0.351	0.085
49	2	3600	0.789	0.223	0.301	103	4	1560	0.617	0.194	0.251
50	2	3600	0.789	0.223	0.223	104	4	1560	0.617	0.194	0.174
51	2	3600	0.789	0.223	0.102	105	4	1560	0.617	0.194	0.085
52	2	3600	0.789	0.122	0.301	106	4	1560	0.617	0.095	0.251
53	2	3600	0.789	0.122	0.223	107	4	1560	0.617	0.095	0.174
54	2	3600	0.789	0.122	0.102	108	4	1560	0.617	0.095	0.085

Table.3 Bid prices and quantities of active load

Bus No.	Blocks (MW@£/MWh)		
	b_1	b_2	b_3
2	2.52@280	1.84@260	1.06@250
3	1.15@260	0.63@250	0.15@230
4	0.03@260	0.02@250	0.01@240
5	9.15@250	6.10@240	3.15@230
6	1.85@240	0.67@230	0.256@230
7	0.93@250	0.56@220	0.41@220
9	0.23@220	0.19@220	0.14@220
10	1.43@220	0.90@210	0.37@200
11	1.52@210	0.89@200	0.44@200
12	0.44@220	0.22@200	0.14@190
13	0.67@200	0.22@190	0.12@170
14	0.37@190	0.14@180	0.07@170

Table.4 Bid prices and quantities of ractive load

Bus No.	Blocks MVAr@£/MVArh		
	b_1	b_2	b_3
2	0.600@200	0.300@230	0.190@200
3	0.210@180	0.120@205	0.060@195
4	0.004@180	0.0035@210	0.0025@200
5	2.110@170	1.200@120	0.430@180
6	0.210@160	0.140@195	0.050@185
7	0.200@170	0.110@185	0.080@175
9	0.060@140	0.030@180	0.020@180
10	0.225@140	0.185@175	0.150@155
11	0.300@135	0.200@155	0.080@160
12	0.080@140	0.070@165	0.030@145
13	0.100@120	0.070@145	0.030@135
14	0.060@115	0.040@153	0.020@130

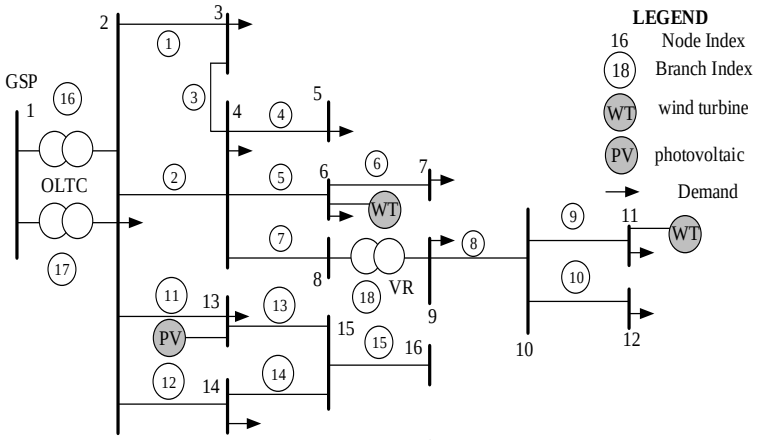

Fig.5. single- line diagram of 16-bus UKGDS

4.1. Calculation of the active power offer prices of WTs and PVs

In order to calculate the active power offer prices of WTs and PVs, financial data of WTs and PVs are summarized in Table 5[47, 50-52]. The annual cost of calculating offer price of WTs and PVs is explained as follows:

$$Ann\_Cost = \frac{r(1+r)^n}{(1+r)^n - 1} \times Inst\_Cost \qquad (33)$$

where n is the depreciation period in year, r is the interest rate in (%), *Inst_Cost* and *Ann_cost* are the installation cost and the annual cost for depreciation, respectively. The capacity factor (the ratio of average power output to the rated power output) is evaluated according to the WTs and PVs data and their capability curve. The active power offer price of WTs and PVs is calculated by dividing the annual cost by the number of equivalent hours.

Table.5 Financial statement for approximating active power offer price of WTs and PVs

Size	WTs	PVs
Installation cost (£/kW)	1200	1400
Number of equivalent hours (h)	4000	4000
Interest rate (%)	3	3
Depreciation time (years)	3	3
Capacity factor (%)	46	46
Annual cost (£/kW-year)	168.81	229.77
Active Offer Price (£/MWh)	**35.16**	**41.03**

4.2. Calculation of the reactive power offer prices of WTs and PVs

According the offer structure of reactive power, a reactive offer prices are listed in Table 6.

Table.6 Reactive power offer prices of WTs and PVs

	Qmax (kVAr)	Qmin KVAr	m_0 (£)	m_1 (£/MVar)	m_2 (£/MVar h)^2	m_{adj} £/MVar	X %
WTs	630	-220	0.082	0.015	0.35×10^{-3}	0.068	30
PVs	270	-60	0.068	0.013	0.42×10^{-3}	0.072	30

5. Simulation Results

In order to investigate the impact of DR program on dispatched active and reactive power, SW and active and reactive D-LMPs, two different cases are taken into account as presented in Table 7. For each case, total dispatched active, reactive power, active and reactive D-LMPs and SW are examined. Figs. 6 and 7 respectively show the total dispatched active and reactive power for cases A and B at each candidate bus. It is seen that the highest and lowest dispatched active and reactive power are related to buses 11 and 13, respectively. This is mainly due to by voltage and thermal constrains at each bus, and active and reactive bid prices. It is evident that in case B, with DR integration, the total active and reactive power dispatched by WTs and PV is higher in comparison with those in case A.

Fig.8 shows the SW for both cases. It is seen that the SW is higher in case B compared to case A. This mainly due to DR integration and the higher dispatched active and reactive power in case B which allows increasing the SW.

The total active and reactive D-LMPs at candidate buses and both cases are shown in Figs. 9 and 10, respectively. The highest active and reactive D-LMPs are related to bus 13 and the lowest active and reactive D-LMPs to bus 11. This is because of the highest and lowest dispatched active and reactive power at these buses. It also observed that the active and reactive D-LMP decreases in case B by implementation DR program.

Table 7. Two cases with and without DR

Case	
A	Without DR
B	With DR

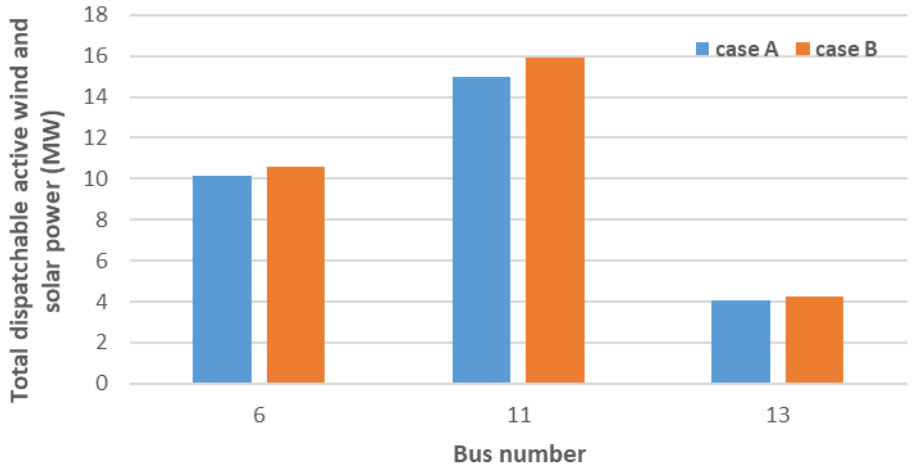

Fig.6. Total dispatched active power at candidate buses

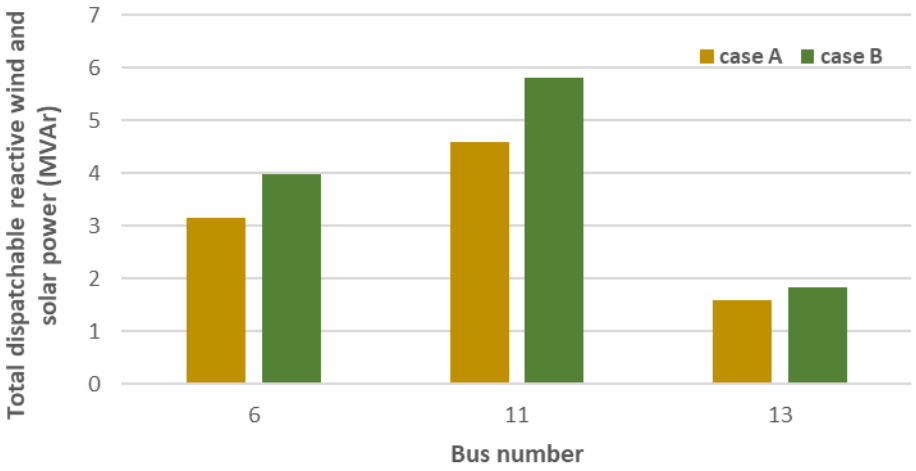

Fig.7. Total dispatched reactive power at candidate buses

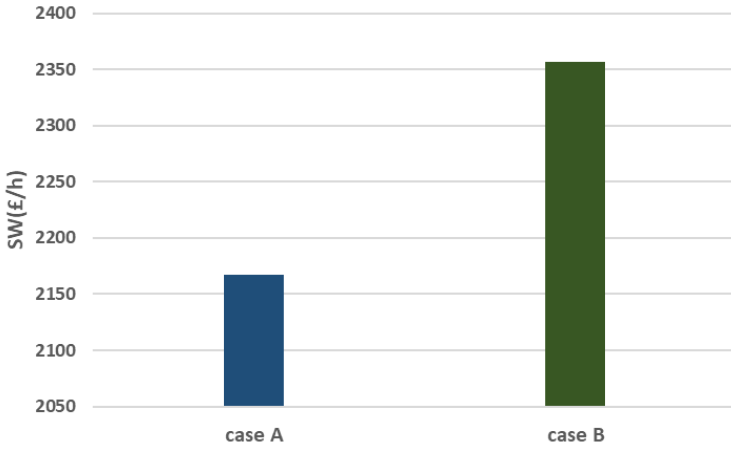

Fig.8. Total social welfare

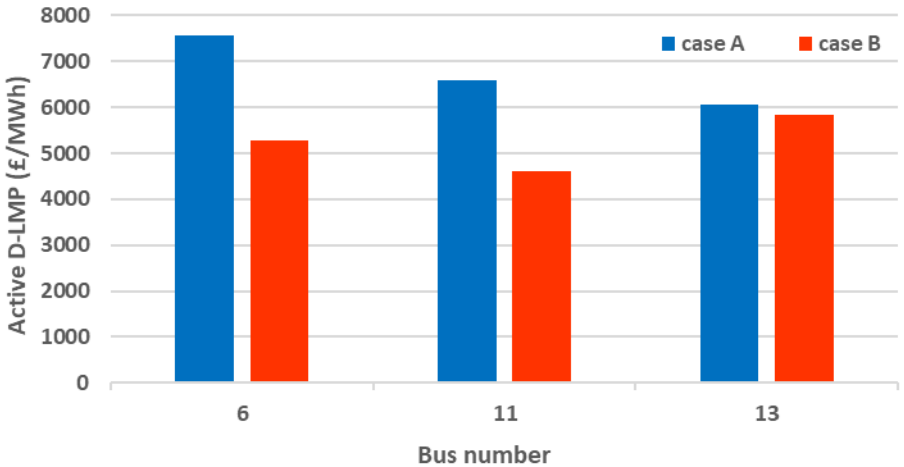

Fig.9.Total active D-LMP at candidate buses

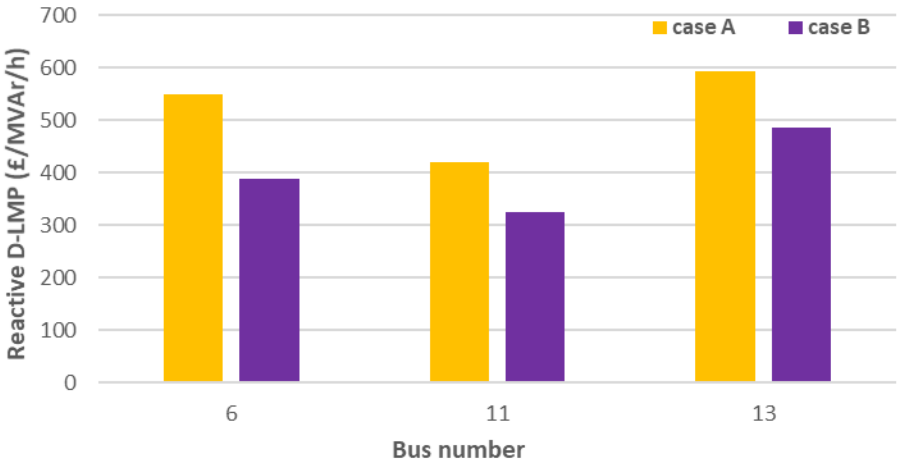

Fig.10. Total reactive D-LMP at candidate buses

6. Conclusion and Futur Work

In this paper, a novel approach for the operation of distribution networks within a joint active and reactive distribution with integration of demand response is proposed. The market-based active and reactive optimal power flow is used to maximize the social welfare in order to determine the optimal capacity of WTs and PVs. In order to evaluate the amount of wind and solar power penetration on the social welfare and on active and reactive locational marginal prices, a stochastic method is used taking into account the uncertainties related to wind speed, solar irradiance and load demand. Scenario-tree is utilized to model the uncertainties.

The proposed method can help distribution network operators to assess the impact of wind and solar power generation penetration on a given network in terms of technical and economic effects. The method will also help DNOs install wind turbines and PVs at more advantageous location in terms of cost reduction and consumers' benefits.

The proposed approach is able to provide an accurate real time pricing which paves the way to operate the proposed market more efficiently thus leads to load demand and prices reduction. This envisages the participation of distribution network operators and active consumers in the distribution market environment, and making use of active and reactive distribution location marginal prices.

The proposed method, which applies in distribution-level market, is also applicable in real distribution networks as shown in [53-55].

In line with this issue, we intend to provide models for active and reactive prices volatility of renewable distributed generators. Moreover, active network management schemes such as coordinated voltage control and adaptive power factor control will be taken into account in the formulation.

Acknowledgment

The authors would like to thank the Ministry of Higher Education and Scientific Research of Iraq for supporting this research work.

References

[1] A. Majzoobi and A. Khodaei, "Application of microgrids in providing ancillary services to the utility grid," *Energy*, vol. 123, pp. 555-563, 2017.

[2] T. Lv and Q. Ai, "Interactive energy management of networked microgrids-based active distribution system considering large-scale integration of renewable energy resources," *Applied Energy*, vol. 163, pp. 408-422, 2016.

[3] M. Alparslan Zehir, A. Batman, A. Ozdemir, A. Font, D. Tsiamitros, D. Stimoniaris, *et al.*, "Impacts of microgrids with renewables on secondary distribution networks," *Applied energy*, 2016.

[4] A. Mahmud, "Large Scale Renewable Power Generation," 2016.

[5] R. H. Zubo, G. Mokryani, H.-S. Rajamani, J. Aghaei, T. Niknam, and P. Pillai, "Operation and planning of distribution networks with integration of renewable distributed generators considering uncertainties: A review," *Renewable and Sustainable Energy Reviews*, vol. 72, pp. 1177-1198, 2017.

[6] R. Palma-Behnke, L. S. Vargas, and A. Jofré, "A distribution company energy acquisition market model with integration of distributed generation and load curtailment options," *IEEE Transactions on Power Systems*, vol. 20, pp. 1718-1727, 2005.

[7] X. Wang, C. Wang, T. Xu, L. Guo, P. Li, L. Yu, *et al.*, "Optimal voltage regulation for distribution networks with multi-microgrids," *Applied Energy*, 2017.

[8] M. Asensio, G. Munoz-Delgado, and J. Contreras, "A bi-level approach to distribution network and renewable energy expansion planning considering demand response," *IEEE Transactions on Power Systems*, 2017.

[9] M. H. Albadi and E. F. El-Saadany, "A summary of demand response in electricity markets," *Electric power systems research*, vol. 78, pp. 1989-1996, 2008.

[10] M. Razmara, G. Bharati, D. Hanover, M. Shahbakhti, S. Paudyal, and R. Robinett III, "Building-to-grid predictive power flow control for demand response and demand flexibility programs," *Applied Energy*, vol. 203, pp. 128-141, 2017.

[11] P. Siano and D. Sarno, "Assessing the benefits of residential demand response in a real time distribution energy market," *Applied Energy*, vol. 161, pp. 533-551, 2016.

[12] S. Pirouzi, J. Aghaei, M. A. Latify, G. R. Yousefi, and G. Mokryani, "A robust optimization approach for active and reactive power management in smart distribution networks using electric vehicles," *IEEE Systems Journal*, 2017.

[13] Y. Lin, J. L. Mathieu, J. X. Johnson, I. A. Hiskens, and S. Backhaus, "Explaining inefficiencies in commercial buildings providing power system ancillary services," *Energy and Buildings*, 2017.

[14] E. L. Miguélez, I. E. Cortés, L. R. Rodríguez, and G. L. Camino, "An overview of ancillary services in Spain," *Electric Power Systems Research*, vol. 78, pp. 515-523, 2008.

[15] R. Doherty, G. Lalor, and M. O'Malley, "Frequency control in competitive electricity market dispatch," *IEEE Transactions on Power Systems*, vol. 20, pp. 1588-1596, 2005.

[16] W. Li, P. Du, and N. Lu, "Design of a New Primary Frequency Control Market for Hosting Frequency Response Reserve Offers from both Generators and Loads," *IEEE Transactions on Smart Grid*, 2017.

[17] J. Suh, D.-H. Yoon, Y.-S. Cho, and G. Jang, "Flexible Frequency Operation Strategy of Power System With High Renewable Penetration," *IEEE Transactions on Sustainable Energy*, vol. 8, pp. 192-199, 2017.

[18] F. Echavarren, E. Lobato, and L. Rouco, "Steady-state analysis of the effect of reactive generation limits in voltage stability," *Electric Power Systems Research*, vol. 79, pp. 1292-1299, 2009.

[19] A. Ahmadimanesh and M. Kalantar, "New Structure of Reactive Power Market by Considering Reactive Power Losses," *Majlesi Journal of Electrical Engineering*, vol. 11, p. 59, 2017.

[20] S. Hasanpour, R. Ghazi, and M. Javidi, "A new approach for cost allocation and reactive power pricing in a deregulated environment," *Electrical Engineering (Archiv fur Elektrotechnik)*, vol. 91, pp. 27-34, 2009.

[21] N. Amjady, A. Rabiee, and H. Shayanfar, "Pay-as-bid based reactive power market," *Energy Conversion and Management*, vol. 51, pp. 376-381, 2010.

[22] H. Ahmadi and A. A. Foroud, "Improvement of the simultaneous active and reactive power markets pricing and structure," *IET Generation, Transmission & Distribution*, vol. 10, pp. 81-92, 2016.

[23] A. C. Rueda-Medina and A. Padilha-Feltrin, "Distributed generators as providers of reactive power support—a market approach," *IEEE Transactions on Power Systems*, vol. 28, pp. 490-502, 2013.

[24] A. Samimi, A. Kazemi, and P. Siano, "Economic-environmental active and reactive power scheduling of modern distribution systems in presence of wind generations: A distribution market-based approach," *Energy Conversion and Management*, vol. 106, pp. 495-509, 2015.

[25] A. N. Celik, "A statistical analysis of wind power density based on the Weibull and Rayleigh models at the southern region of Turkey," *Renewable energy*, vol. 29, pp. 593-604, 2004.

[26] S. S. Reddy, A. Abhyankar, and P. Bijwe, "Market clearing for a wind-thermal power system incorporating wind generation and load forecast uncertainties," in *Power and Energy Society General Meeting, 2012 IEEE*, 2012, pp. 1-8.

[27] G. Mokryani, "Active distribution networks operation within a distribution market environment," in *Sustainable Development in Energy Systems*, ed: Springer, 2017, pp. 107-118.

[28] Y. M. Atwa and E. F. El-Saadany, "Probabilistic approach for optimal allocation of wind-based distributed generation in distribution systems," *IET Renewable Power Generation*, vol. 5, pp. 79-88, 2011.

[29] S. S. Reddy, B. Panigrahi, R. Kundu, R. Mukherjee, and S. Debchoudhury, "Energy and spinning reserve scheduling for a wind-thermal power system using CMA-ES with mean learning technique," *International Journal of Electrical Power & Energy Systems*, vol. 53, pp. 113-122, 2013.

[30] S. S. Reddy and J. A. Momoh, "Realistic and transparent optimum scheduling strategy for hybrid power system," *IEEE Transactions on Smart Grid*, vol. 6, pp. 3114-3125, 2015.

[31] G. Mokryani, A. Majumdar, and B. C. Pal, "Probabilistic method for the operation of three-phase unbalanced active distribution networks," *IET Renewable Power Generation*, vol. 10, pp. 944-954, 2016.

[32] S. Montoya-Bueno, J. Muñoz-Hernández, and J. Contreras, "Uncertainty management of renewable distributed generation," *Journal of Cleaner Production*, vol. 138, pp. 103-118, 2016.

[33] J. Widén, "Correlations between large-scale solar and wind power in a future scenario for Sweden," *IEEE transactions on sustainable energy*, vol. 2, pp. 177-184, 2011.

[34] S. S. Reddy, P. Bijwe, and A. R. Abhyankar, "Joint energy and spinning reserve market clearing incorporating wind power and load forecast uncertainties," *IEEE Systems Journal*, vol. 9, pp. 152-164, 2015.

[35] S. S. Reddy, P. Bijwe, and A. R. Abhyankar, "Optimal posturing in day-ahead market clearing for uncertainties considering anticipated real-time adjustment costs," *IEEE Systems Journal*, vol. 9, pp. 177-190, 2015.

[36] G. Mokryani, Y. F. Hu, P. Pillai, and H.-S. Rajamani, "Active distribution networks planning with high penetration of wind power," *Renewable Energy*, vol. 104, pp. 40-49, 2017.

[37] S. Montoya-Bueno, J. I. Muoz, and J. Contreras, "A stochastic investment model for renewable generation in distribution systems," *IEEE Transactions on Sustainable Energy*, vol. 6, pp. 1466-1474, 2015.

[38] G. Muñoz-Delgado, J. Contreras, and J. M. Arroyo, "Multistage generation and network expansion planning in distribution systems considering uncertainty and reliability," *IEEE Transactions on Power Systems*, vol. 31, pp. 3715-3728, 2016.

[39] M. Asensio, P. M. de Quevedo, G. Munoz-Delgado, and J. Contreras, "Joint Distribution Network and Renewable Energy Expansion Planning considering Demand Response and Energy Storage–Part I: Stochastic Programming Model," *IEEE Transactions on Smart Grid*, 2016.

[40] L. Baringo and A. Conejo, "Correlated wind-power production and electric load scenarios for investment decisions," *Applied energy*, vol. 101, pp. 475-482, 2013.

[41] C. Cecati, C. Citro, and P. Siano, "Combined operations of renewable energy systems and responsive demand in a smart grid," *IEEE Transactions on Sustainable Energy*, vol. 2, pp. 468-476, 2011.

[42] T. El-Fouly, H. Zeineldin, E. El-Saadany, and M. Salama, "Impact of wind generation control strategies, penetration level and installation location on electricity market prices," *IET Renewable Power Generation*, vol. 2, pp. 162-169, 2008.

[43] S. S. Reddy, A. Abhyankar, and P. Bijwe, "Reactive power price clearing using multi-objective optimization," *Energy*, vol. 36, pp. 3579-3589, 2011.

[44] S. Haffner, L. F. A. Pereira, L. A. Pereira, and L. S. Barreto, "Multistage model for distribution expansion planning with distributed generation—Part I: Problem formulation," *IEEE Transactions on Power Delivery*, vol. 23, pp. 915-923, 2008.

[45] S. F. Santos, D. Z. Fitiwi, A. W. Bizuayehu, M. Shafie-Khah, M. Asensio, J. Contreras, *et al.*, "Impacts of Operational Variability and Uncertainty on Distributed Generation Investment Planning: A Comprehensive Sensitivity Analysis," *IEEE Transactions on Sustainable Energy*, vol. 8, pp. 855-869, 2017.

[46] "Distibuted Generation and Sustainable Electrical Energy Center,United Kingdom Generic Distribution System (UK GDS). [Online]." *Available* <*http://www.sedg.ac.uk/*>.
[47] A. G. Tsikalakis and N. D. Hatziargyriou, "Centralized control for optimizing microgrids operation," in *Power and Energy Society General Meeting, 2011 IEEE*, 2011, pp. 1-8.
[48] P. Siano and G. Mokryani, "Assessing wind turbines placement in a distribution market environment by using particle swarm optimization," *IEEE Transactions on Power Systems*, vol. 28, pp. 3852-3864, 2013.
[49] A. Brooke, D. Kendrick, A. Meeraus, R. Raman, and U. America, "The general algebraic modeling system," *GAMS Development Corporation*, vol. 1050, 1998.
[50] P. Siano and G. Mokryani, "Evaluating the benefits of optimal allocation of wind turbines for distribution network operators," *IEEE Systems Journal*, vol. 9, pp. 629-638, 2015.
[51] G. Mokryani and P. Siano, "Strategic placement of distribution network operator owned wind turbines by using market-based optimal power flow," *IET Generation, Transmission & Distribution*, vol. 8, pp. 281-289, 2014.
[52] G. Mokryani, Y. F. Hu, P. Papadopoulos, T. Niknam, and J. Aghaei, "Deterministic approach for active distribution networks planning with high penetration of wind and solar power," *Renewable Energy*, vol. 113, pp. 942-951, 2017.
[53] G. Mokryani and P. Siano, "Combined Monte Carlo simulation and OPF for wind turbines integration into distribution networks," *Electric Power Systems Research*, vol. 103, pp. 37-48, 2013.
[54] G. Mokryani and P. Siano, "Evaluating the integration of wind power into distribution networks by using Monte Carlo simulation," *International Journal of Electrical Power & Energy Systems*, vol. 53, pp. 244-255, 2013.
[55] P. Siano and G. Mokryani, "Probabilistic assessment of the impact of wind energy integration into distribution networks," *IEEE Transactions on Power Systems*, vol. 28, pp. 4209-4217, 2013.